

# Adult Human Retinal Neurons in Culture: Physiology of Horizontal Cells

Serge Picaud, David Hicks, Valérie Forster, José Sabel, and Henri Dreyfus

**PURPOSE.** Adult postmortem human retinal neurons in long-term monolayer cultures were recorded to characterize the voltage- and transmitter-gated currents in putative human horizontal cells (HCs).

**METHODS.** Enzymatically and mechanically dissociated human retinal cells were seeded on polylysine and laminin-coated coverslips. Cells were identified by immunocytochemistry with cell type-specific antibodies and recorded with the patch-clamp technique.

**RESULTS.** Immunostaining and responses to voltage steps confirmed the survival of various retinal cell types. Horizontal cells were identified by their specific glutamate-modulated anomalous rectifier  $K^+$  current conductance. This identification was further confirmed by subsequent immunolabeling of dye-labeled recorded cells with an anti-parvalbumin antibody that selectively stained HCs in frozen human retinal sections. Horizontal cells generated voltage-gated currents classically observed in HCs from fish to mammals: a transient outward  $K^+$  current, a sustained outward  $K^+$  current, and an L-type  $Ca^{2+}$  current.  $Na^+$  currents were observed in only a few HCs. As in other species, glutamate,  $\gamma$ -aminobutyric acid (GABA), and glycine generated responses mediated by the activation of kainate/(RS)- $\alpha$ -amino-3-hydroxy-5-methyl-4-isoxazolepropionic acid (AMPA), GABA<sub>A</sub>, and glycine receptors, respectively.

**CONCLUSIONS.** Various human retinal cell populations survive in vitro as indicated by immunolabeling with specific cell markers and by the diversity of responses to voltage steps. Human HCs exhibited extensive physiological similarities to HCs from other vertebrate species and a maintained expression of parvalbumin. These results constitute a comprehensive analysis of voltage- and transmitter-gated currents in a primate retinal neuron and validate the use of long-term monolayer culture of adult human neurons as a novel in vitro model for the study of human vision. (*Invest Ophthalmol Vis Sci*. 1998;39:2637-2648)

To understand the molecular and cellular mechanisms of signal processing of visual information in the vertebrate retina, transmitter- and voltage-gated conductances have to date been analyzed in retinal neurons from different classes. However, the lack of appropriate preparations has prevented such a physiological analysis in primate retinal neurons. This statement applies, for example, to horizontal cells (HCs), interneurons that are considered to mediate lateral interactions participating in increasing contrast at object edges, adjusting light sensitivity,<sup>1</sup> and participating in color coding.<sup>2</sup>

Horizontal cells classically express five different voltage-gated currents: a  $Na^+$  current, an anomalous rectifier  $K^+$  current, a transient outward  $K^+$  current, a delayed rectifier  $K^+$  current, and an L-type  $Ca^{2+}$  current (fish,<sup>3-6</sup> turtles,<sup>7</sup> cats,<sup>8</sup> and rab-

bits<sup>9,10</sup>). Responses to the major retinal transmitters glutamate, glycine, and  $\gamma$ -aminobutyric acid (GABA) have been recorded in lower vertebrates and rabbits. However, the molecular mechanisms underlying these responses appear to be species-dependent, which underlines the need to characterize these responses in primate and human retinal cells. For instance, only fish HCs produced GABA-stimulated or glutamate-stimulated responses that involved GABA<sub>C</sub> receptors,<sup>11,12</sup> GABA transporters,<sup>13,14</sup> or N-methyl-D-aspartate (NMDA) receptors.<sup>15</sup> Similarly, isolated rabbit HCs did not respond to glycine applications<sup>16</sup> as did HCs from fish<sup>17</sup> and salamanders.<sup>18,19</sup>

In the primate retina, the morphologic distinction between the two HC types (HI, HII) is less clear than in other mammals because they have similar sizes and both bear an axon that contacts either cones (HII) or rods (HI); dendrites remain connected only to cones.<sup>20</sup> In the human retina, a third type (HIII) was subdivided from the HI type on the basis of its dendritic field shape and number of cone contacts.<sup>21</sup> Primate HCs were recently shown in isolated retinae to lack a spectral "opponency" despite their cone selectivity.<sup>22</sup>

Adult human postmortem retinal neurons<sup>23-26</sup> have been reported to survive for long periods of time in culture and to redevelop neurites. Because cell culture has been used with success to investigate the physiology of several retinal cell types in lower vertebrates,<sup>27</sup> we have examined whether monolayer cultures of adult postmortem human retinal cells could provide an adequate in vitro preparation for analysis of molecular and cellular mechanisms in primate vision. Using

From the Laboratoire de Physiopathologie Rétinienne, INSERM CJF 92/02, Université Louis Pasteur, Strasbourg, France.

Supported by grants from DRET/DGA, la Fédération des Aveugles de France, la Fondation de l'Avenir, and la Fondation de France, MGEN/INSERM. SP was supported by l'Association pour l'Aide au Développement de la Recherche sur la régénération de la rétine et sa Transplantation (ADRET-Alsace, Strasbourg, France) and IRIS Servier (Paris, France). The Conseil Régional d'Alsace, Conseil Général du Bas Rhin and Communauté Urbaine de Strasbourg provided the electro-physiological equipment.

Submitted for publication April 2, 1998; revised July 10, 1998; accepted August 21, 1998.

Proprietary interest category: N.

Reprint requests: Serge Picaud, INSERM CJF 92/02, Médicale A, BP426, 1 place de l'hôpital, 67091 Strasbourg Cedex, France.

immunolabeling and patch-clamp recording, we demonstrated, and will report here, the persistence of the major neuronal cell types in these cultures and, subsequently, focused our analysis on voltage- and transmitter-gated currents in putative human HCs.

## MATERIALS AND METHODS

### Cell Culture

Cell cultures were prepared as described previously.<sup>26</sup> Human ocular tissue was obtained from the Blood Transfusion Center-Eye Bank of Franche-Comté from five donors (ranging in age from 45 to 83 years) subsequent to death through natural causes. Corneal tissue was removed for grafts, and the posterior eyecup with lens and vitreous attached was stored within 10 to 24 hours in cold CO<sub>2</sub>-independent Dulbecco's modified Eagle's medium (DMEM; GIBCO, Life Technologies, Paisley, UK) and shipped to our laboratory. Postmortem delay times were always less than 48 hours before cell culture preparation. Retinae separated from the posterior eyecup were placed in warm DMEM-Ham's F-12 (DMEM/F-12, GIBCO) and chopped into small fragments (~2 mm<sup>2</sup>). The fragments were then washed twice in warm mammalian Ringer's solution without Ca<sup>2+</sup> and supplemented with 0.1 mM EDTA. They were incubated with 0.2% activated papain (Worthington, Freehold, NJ) for 15 to 20 minutes at 37°C. Digestion was arrested by the addition of the same volume of DMEM/F-12 containing 10% fetal calf serum (DMEM/FCS; GIBCO), 0.1 mg/ml DNase1, and 1 mg/ml bovine serum albumin. The fragments were dissociated by gentle trituration using flame-polished Pasteur pipettes. After mild centrifugation, cells were resuspended in DMEM/FCS, an aliquot was incubated with trypan blue vital dye and examined on a hemocytometer to ascertain cell number and viability. Cells were seeded at an initial density of approximately 10<sup>6</sup> cells/cm<sup>2</sup> into 24-well tissue-culture plates containing coverslips precoated with polylysine and laminin. Culture medium was renewed weekly, and such cultures could be maintained for at least 3 months in vitro. Recordings were performed between 6 and 69 days in culture.

### Recordings

Recording pipettes were pulled from thin-walled borosilicate glass (model TW150F; World Precision Instruments, Sarasota, FL) using a Brown and Flaming type puller (model P-87; Sutter Instruments, Novato, CA). Pipettes had a measured resistance in Ringer's solution of 5 MΩ to 10 MΩ and a series resistance during recordings estimated at 14.8 ± 0.7 MΩ (±SEM, n = 15). A patch-clamp amplifier (model RK400; Biologic, Grenoble, France) was used to voltage-clamp the recorded cells. The liquid junction potentials were corrected using a procedure previously described.<sup>28</sup> Data were filtered at 3 kHz and digitized at either 10 kHz during voltage-step experiments or 1 Hz during transmitter applications using a data acquisition Labmaster board (Scientific Solutions, Solon, OH) mounted to an IBM-compatible personal computer. Experimental data were acquired and analyzed using the Patchit and Tack software packages, respectively.<sup>29</sup> All data reported in this article were reproduced on at least three different cells.

### Solutions and Drug Application

The standard recording solution contained (in mM) 135 NaCl, 5 KCl, 1 CaCl<sub>2</sub>, 1 MgCl<sub>2</sub>, 10 glucose, and 5 HEPES and was

titrated to pH 7.75 by the addition of NaOH. For measuring the Ca<sup>2+</sup> current, the solution contained (in mM) 5 CsCl<sub>2</sub>, 10 4-aminopyridine (4-AP), 30 tetraethylammonium (TEA), 90 NaCl, 5 KCl, 10 CaCl<sub>2</sub>, 1 MgCl<sub>2</sub>, 10 glucose, and 5 HEPES and was titrated to pH 7.75 by the addition of HCl. Blocking Ca<sup>2+</sup> currents was achieved by substituting 4 mM CoCl<sub>2</sub> for CaCl<sub>2</sub> in this solution. In the high K<sup>+</sup> solution, 35 mM KCl was substituted for an equimolar concentration of NaCl.

Drugs were usually added to these solutions unless specified in the text without substitution. They were applied to the cells with a local perfusion system driven by gravity and controlled by the computer via electrovalves (NR, West Cadwell, NJ). Fine propylene tubing from eight reservoirs converged to a plastic pipette tip (300 μm id) that was placed approximately 500 μm away from the recorded cell. The flow rate of the local perfusion system was ~0.17 ml/min. To improve the wash of drugs, a bath perfusion system, also driven by gravity, was constantly flowing at a rate of 2 ml/min.

The pipette solution used in most whole-cell recordings contained (in mM) 140 KCl, 1 MgCl<sub>2</sub>, 0.5 EGTA, 5 ATP (disodium), and 4 HEPES and was adjusted to pH 7.4 with KOH. The Ca<sup>2+</sup> currents were measured using a solution with a calculated Cl<sup>-</sup> equilibrium potential (E<sub>Cl</sub>) of -30 mV. In this solution, 86 mM K-gluconate and 5 mM BAPTA (tetrapotassium) were substituted for 96 mM KCl and 0.5 EGTA. In all recording solutions, 0.05% to 0.1% of either Lucifer yellow or sulforhodamine 101 (SR101) was added to stain the recorded cells.

### Immunocytochemistry

The general procedure for immunolabeling was as previously described.<sup>30</sup> Antibodies used on cultured cells were initially screened on frozen sections of postmortem human retinae, which were prepared from small samples removed from the retinae before culture. Cells were fixed in 4% paraformaldehyde in phosphate-buffered saline (PBS) at 4°C during 1 hour. Then they were rinsed in PBS, permeabilized 5 minutes in PBS containing 0.1% Triton X-100, and pretreated with PBS containing 0.1% bovine serum albumin, 0.1% Tween-20, and 0.1% NaN<sub>3</sub> for 15 minutes to reduce nonspecific binding. Incubation with the primary monoclonal or polyclonal antibody lasted for 1 to 2 hours at room temperature. The antibodies used in the present study were anti-arrestin polyclonal antibody (a generous gift from Igal Gery, NIH, Bethesda, MD) specific for rod and cone photoreceptors<sup>31</sup>; anti-protein kinase C monoclonal antibody (Amersham, Les Ulis, France) specific for rod bipolar cells<sup>32,33</sup>; anti-parvalbumin monoclonal antibody (ICN Immunobiologicals, Lisle, IL), which labels principally HCs in the primate retina<sup>34</sup>; anti-syntaxis monoclonal antibody (a generous gift from Colin Barnstable, Yale University, CT) specific for amacrine cells<sup>35</sup>; anti-neurofilament (heavy chain) monoclonal antibody (a generous gift from Colin Barnstable, Yale University), which labels HCs and ganglion cells<sup>36</sup>; and anti-neuron-specific enolase polyclonal antibody (Cambridge Research Biochemicals, Wilmington, DE), which binds to all retinal neurons.<sup>30</sup> After washing, cells were treated sequentially with biotinylated anti-mouse or anti-rabbit IgG antibody (Amersham; 10 μg/ml for 1 hour), with the choice depending on the primary antibody (mouse monoclonal or rabbit polyclonal). Labeled cells were revealed with either ExtrAvidin conjugated to tetrarhodamine isothiocyanate (ExAv-TRITC) or fluorescein isothiocyanate (ExAv-FITC; 10 μg/ml for 1 hour; Sigma-Aldrich, St. Louis, MO).

## Cell Observation

During recordings, cells were observed under a Nikon Optiphot 2 microscope equipped with a fixed stage, Nomarski optics, and a water-immersion objective 40 $\times$ /0.55W (160/-; Nikon, Tokyo, Japan). Fluorescent labelings were observed using a Nikon Optiphot 2 microscope under epifluorescence illumination (SR101 or TRITC: interference filter 510–560 nm, dichroic mirror DM575, barrier filter BA590; Lucifer yellow: interference filter 425DF45, dichroic mirror XF14, barrier filter BA520; FITC: interference filter 470 nm to 490 nm, dichroic mirror XF22, barrier filter 530DF30).

## Chemicals and Proteins

All chemicals and enzymes for which the source was not provided above were obtained from Sigma, except for (RS)- $\alpha$ -amino-3-hydroxy-5-methyl-4-isoxazolepropionic acid (AMPA); Tocris Neuramin, Bristol, UK) and 6-cyano-7-nitro quinoxaline-2,3-dione (CNQX; Research Biochemicals, Natick, MA).

## RESULTS

### Cell Diversity

Examination of cultures revealed scattered rounded neurons overlying numerous glial cells. Numbers of surviving neurons varied among individual experiments, but an estimated  $2 \times 10^4$  neurons per well were present after 2 weeks in culture. In such cultures, several cell populations were identified on the basis of their immunolabeling with specific antibody markers for rod and cone photoreceptors (Fig. 1A), bipolar cells (Fig. 1B), amacrine cells (Fig. 1C), ganglion cells (Fig. 1D), and HCs (Figs. 1E, 1F). These different cell types maintained different morphologic features. As previously shown,<sup>25,26</sup> cones had large spindle-shaped cell bodies ( $14.4 \pm 0.9 \mu\text{m}$ ,  $n = 9$ ) with thick dendrites, whereas rods had small round cell bodies ( $8.5 \pm 0.3 \mu\text{m}$ ,  $n = 39$ ) with thin dendrites. Rod bipolar cells usually preserved their bipolar configuration with a large irregular cell body ( $17.0 \pm 0.6 \mu\text{m}$ ,  $n = 7$ ). Horizontal and amacrine cells had cell bodies of a similar size ( $12.3 \pm 0.3 \mu\text{m}$ ,  $n = 20$  and  $12.7 \pm 0.6 \mu\text{m}$ ,  $n = 22$ , respectively). Amacrine cells were often stellate-shaped with numerous ramified dendrites, whereas HCs usually appeared round with a few thick processes. Ganglion cells were always larger with an extended ramification (cell bodies:  $22.2 \pm 0.9 \mu\text{m}$ ,  $n = 7$ ). This diversity of human retinal neurons in culture was corroborated by the variety of responses to voltage steps when recorded with the patch-clamp technique in the whole-cell configuration (Fig. 2). It is clear that some cells expressed a transient inward current (Figs. 2C, 2E, 2F), presumably a  $\text{Na}^+$  current, in contrast to others (Figs. 2A, 2B, 2D). The presence of a sustained inward current at potential more negative than  $-80 \text{ mV}$  (Figs. 2A, 2D, 2E) also provided a differentiating feature between certain cell populations.

### Identification of HCs

Cells with a morphology similar to that of HCs, round cell body and relatively thick processes, generated a large inward current activated during voltage steps to potentials more negative than the holding potential of  $-70 \text{ mV}$  (Fig. 2D). This current was blocked by 5 mM  $\text{Cs}^{2+}$  or 0.5 mM  $\text{Ba}^{2+}$  (Figs. 3A, 3B). When the  $\text{K}^+$  concentration was increased from 5 mM to 10 mM, this

$\text{Cs}^{2+}$ -sensitive current increased in amplitude (5 mM  $\text{K}^+$ :  $I = -190 \pm 31 \text{ pA}$ ; 10 mM  $\text{K}^+$ :  $I = -270 \pm 47 \text{ pA}$  at  $-120 \text{ mV}$ ,  $n = 7$ ), and the potential of activation (or reversion) followed the  $\text{K}^+$  equilibrium potential (5 mM  $\text{K}^+$ :  $E_K = -84 \text{ mV}$ ;  $E_{rev} = -82.6 \pm 1.8 \text{ mV}$ ,  $n = 9$ ; 10 mM  $\text{K}^+$ :  $E_K = -66 \text{ mV}$ ,  $E_{rev} = -60.9 \pm 2.9 \text{ mV}$ ,  $n = 8$ ). These current characteristics are typical for the  $\text{K}^+$  anomalous rectifier current found in HCs from fish,<sup>3–6</sup> turtles<sup>7</sup> or cats.<sup>8</sup> In the retina, the anomalous rectifier  $\text{K}^+$  current can even be considered as an electrophysiological signature for HCs because it has been identified solely in this cell type.<sup>27</sup> These cells had a membrane capacitance ranging from 8.9 pF to 39 pF ( $19.2 \pm 1.1 \text{ pF}$ ,  $n = 48$ ) consistent with the small size reported for primate HCs.

Electrophysiological identification of HC was confirmed using an anti-parvalbumin antibody to identify human HCs in culture (Figs. 1E, 1F). On frozen sections of human retina, the anti-parvalbumin antibody labeled intensely the outer plexiform layer (OPL) and a cell population at the scleral surface of the inner nuclear layer (INL; Figs. 1G, 1H, 1I) where HCs and their processes are located. Therefore, this antibody was used to identify HCs in cultures of human retinal cells despite the light staining observed in cell bodies of the ganglion cell layer. Parvalbumin-immunoreactive neurons accounted for 24% (345 from a sample of 1446 neurons double-immunolabeled with polyclonal anti-neuron-specific enolase antibody) of total neurons at 10 weeks in culture. These putative HCs in vitro possessed a relatively small and round cell body with few large neurites extending up to  $100 \mu\text{m}$ , a morphology that was used to localize HCs before the recording.

During their recording, human retinal cells in culture were labeled with the dye, SR101, introduced in the recording pipette solution (Fig. 4). The culture was then fixed and stained with the anti-parvalbumin antibody. Recorded cells expressing the anomalous rectifier  $\text{K}^+$  current were parvalbumin positive (Fig. 4C,  $n = 5$ ), whereas other recorded cells were not parvalbumin immunoreactive (data not shown). Although SR101 produced a dim fluorescence using the FITC filter combination, a clear distinction could be made between FITC immunostaining and this SR101 fluorescence (Figs. 4G, 4H). To confirm the cellular identification, recorded cells were also stained with Lucifer yellow (Fig. 4E), which did not generate a signal with the TRITC filter combination such that the culture could be immunolabeled with the anti-parvalbumin antibody using TRITC as the fluorochrome. Cells expressing the anomalous rectifier  $\text{K}^+$  current were again double-labeled (Fig. 4F,  $n = 4$ ), whereas other neurons were immunonegative. Figures 4E and 4F also illustrate that Lucifer yellow and the immunolabeling were distributed differently in the recorded cells. Because the immunostaining varied in intensity from cell to cell, it was possible that lightly labeled cells represented ganglion cells that appeared lightly labeled with the anti-parvalbumin antibody in retinal sections (Fig. 1H). However, recorded ganglion cells identified by an anti-neurofilament immunolabeling (Figs. 4G, 4H) exhibited a very different cell morphology and very different responses to voltage steps, showing for instance robust  $\text{Na}^+$  inward currents as illustrated in Figure 2F. The light anti-parvalbumin antibody staining was interpreted instead as washout of cytosolic parvalbumin during the recording. This immunocytochemical labeling was consistent with our conclusion that human retinal cells expressing anomalous rectifier  $\text{K}^+$  current belong to the HC population.

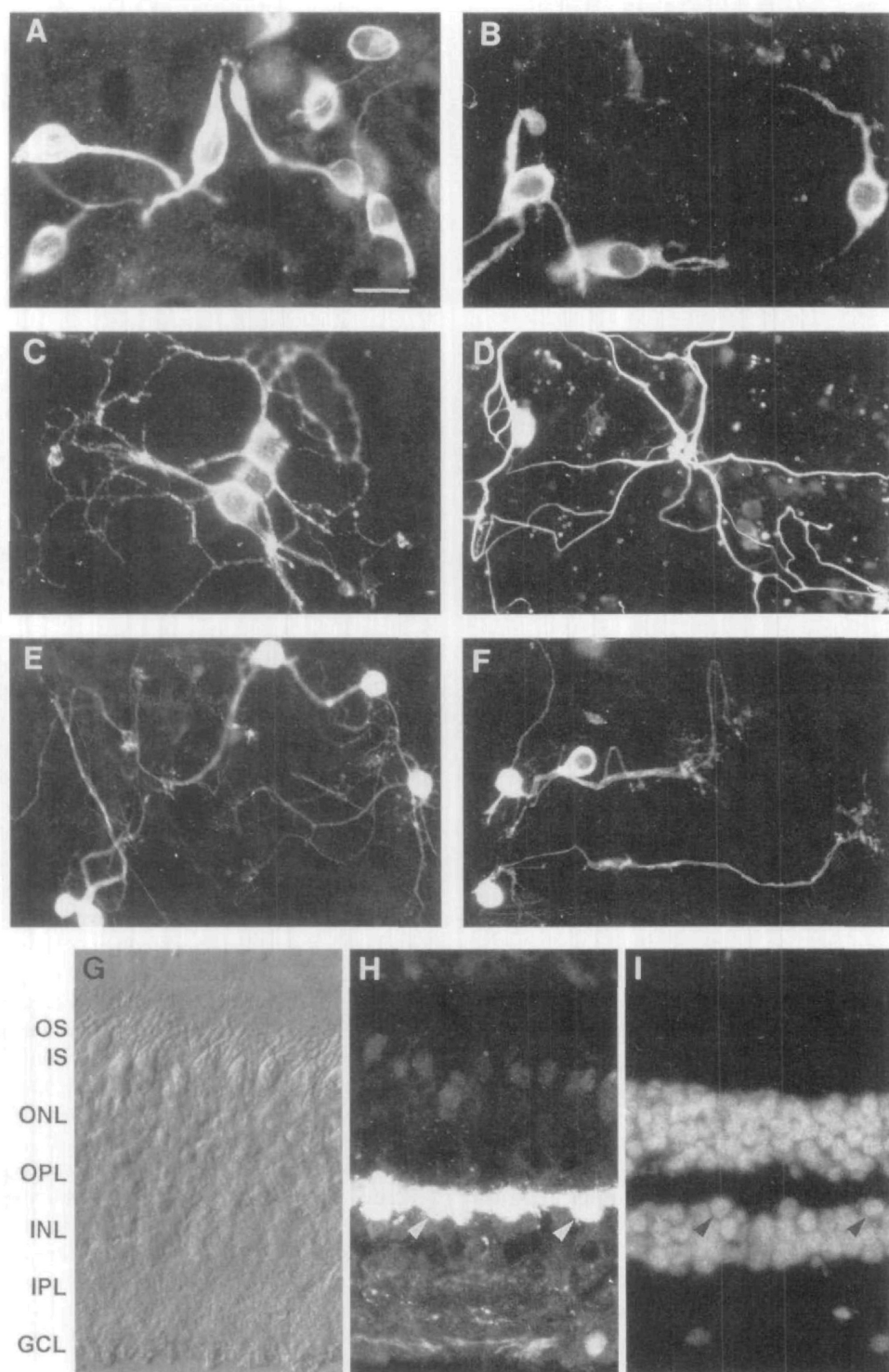


**FIGURE 1.** Immunocytochemical identification of adult human retinal cells in culture (**A**, **B**, **C**, **E**, **F**) or *in situ* (**G**, **H**, **I**). (**A**) Photoreceptors stained with anti-arrestin antibody. Considering the diameter of the cell bodies (~8  $\mu\text{m}$ ), the immunoreactive cells illustrated here are likely rods. (**B**) Rod bipolar cells labeled with anti-protein kinase C antibody. (**C**) Amacrine cells stained with anti-syntaxin antibody. (**D**) Ganglion cells labeled with anti-neurofilament antibody. (**E**, **F**) Horizontal cells stained with anti-parvalbumin antibody. (**G**, **H**, **I**) Retinal section observed by Nomarski differential interference contrast (**G**) and stained with either anti-parvalbumin antibody (**H**) or the dye 4'6-diamidino-2-phenylindole-2HCl (DAPI; **I**). The intense staining of the outer plexiform layer (OPL) and the outer part of the inner nuclear layer (INL) is consistent with a selective labeling of horizontal cells. *Arrowheads* point to parvalbumin-immunopositive cell bodies (**H**) and their DAPI-stained nuclei located in the outer part of the INL (**I**). GCL, ganglion cell layer; IPL, inner plexiform layer; ONL, outer nuclear layer; IS, inner segment; OS, outer segment. Scale bar, (**A**, **B**, **C**) 13  $\mu\text{m}$ ; (**D**, **E**, **F**) 26  $\mu\text{m}$ ; and (**G**, **H**, **I**) 20  $\mu\text{m}$ .

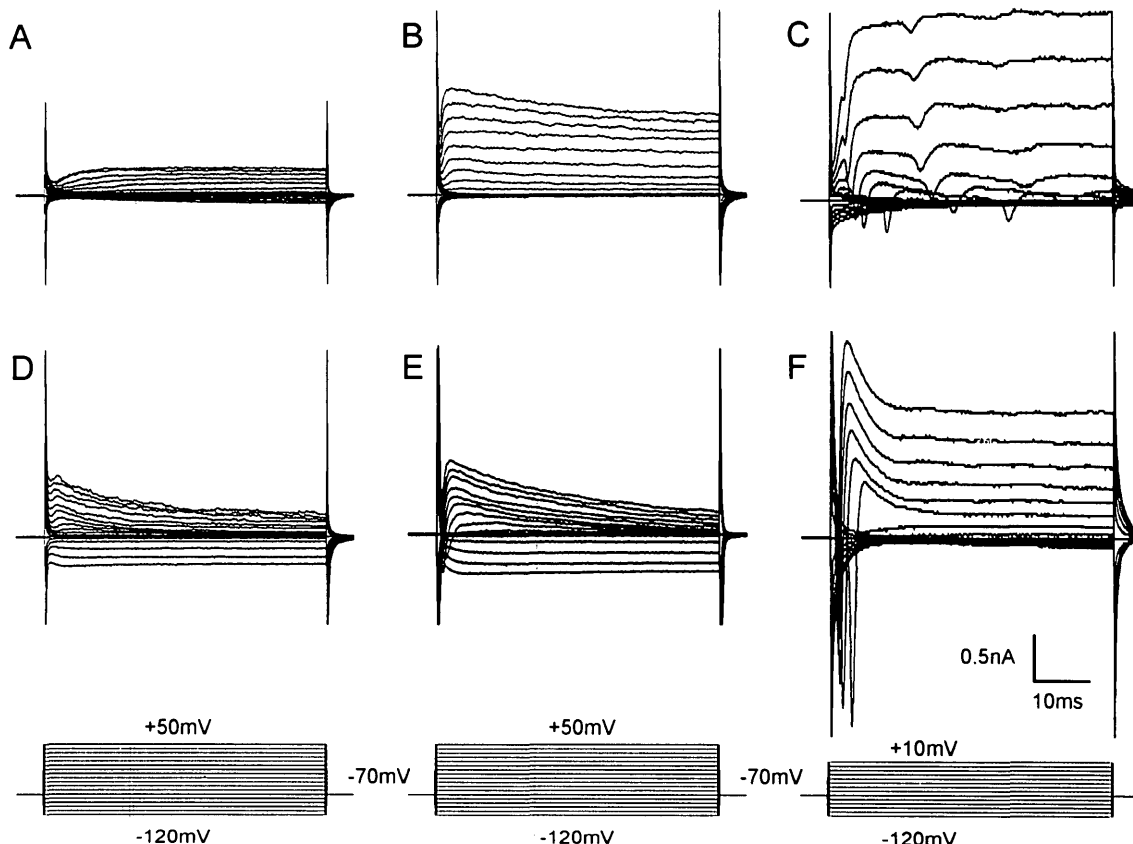


**FIGURE 2.** Diversity of responses to voltage steps in cultured human retinal cells. Cells were voltage-clamped at  $-70$  mV, and voltage steps were applied in 10-mV increments, from  $-120$  mV to either  $+50$  mV (**A, B, D, E**) or  $+10$  mV (**C, F**). All recordings are illustrated at the same scale to demonstrate the difference in cell responses. Note, for instance, the transient inward current in (**E**), (**C**), and (**F**).

### Transient Outward $K^+$ Current

Human HCs in culture expressed a transient outward  $K^+$  current (Fig. 5A) sensitive to 4-AP applied in the bathing solution. Whole-cell currents were measured in the absence or presence of 10 mM 4-AP (Fig. 5A), while the inward anomalous rectifier  $K^+$  current was suppressed with 5 mM  $Cs^{2+}$ . The transient outward current was calculated by subtracting the cellular currents recorded in these two conditions (Fig. 5A,

inset). The 4-AP-sensitive current was observed at potentials more positive than  $-50$  mV, and its amplitude increased linearly with the voltage command (Fig. 5A, circle). The voltage-dependent inactivation of the 4-AP-sensitive current was measured at  $+50$  mV after a 1-second conditioning stimulus at potentials ranging from  $-120$  mV to  $+50$  mV in 10-mV increments. The current amplitude at  $+50$  mV decreased when increasing the conditioning potential; the current inactivated

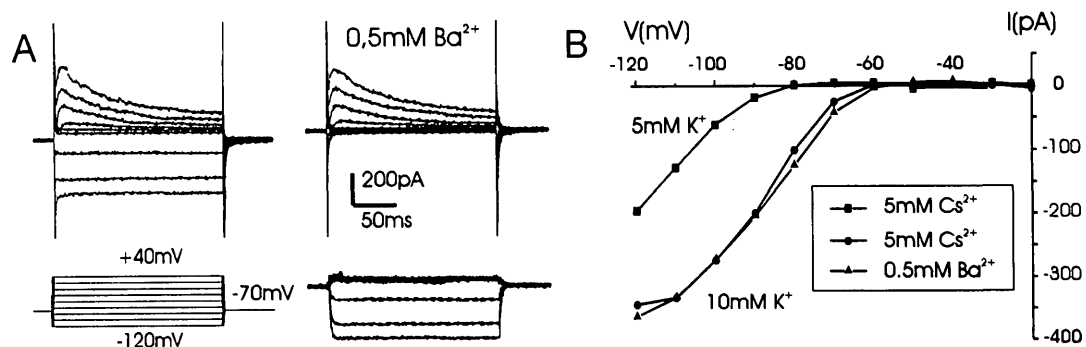


**FIGURE 3.** The inward anomalous rectifier  $K^+$  current, an electrophysiological signature for human horizontal cells. (**A**) Cellular currents were measured in the absence or presence of  $Ba^{2+}$  ( $0.5$  mM) during voltage steps applied from a holding voltage of  $-70$  mV to potentials ranging from  $-120$  mV to  $+40$  mV in 20-mV increments. The difference between these measurements represents the  $Ba^{2+}$ -suppressed current. (**B**) Current-voltage (IV) curve of the currents suppressed by either  $Ba^{2+}$  or  $Cs^{2+}$  from the cell shown in (**A**). The currents suppressed by  $Cs^{2+}$  were measured in the presence of  $K^+$  concentrations of  $5$  mM and  $10$  mM.

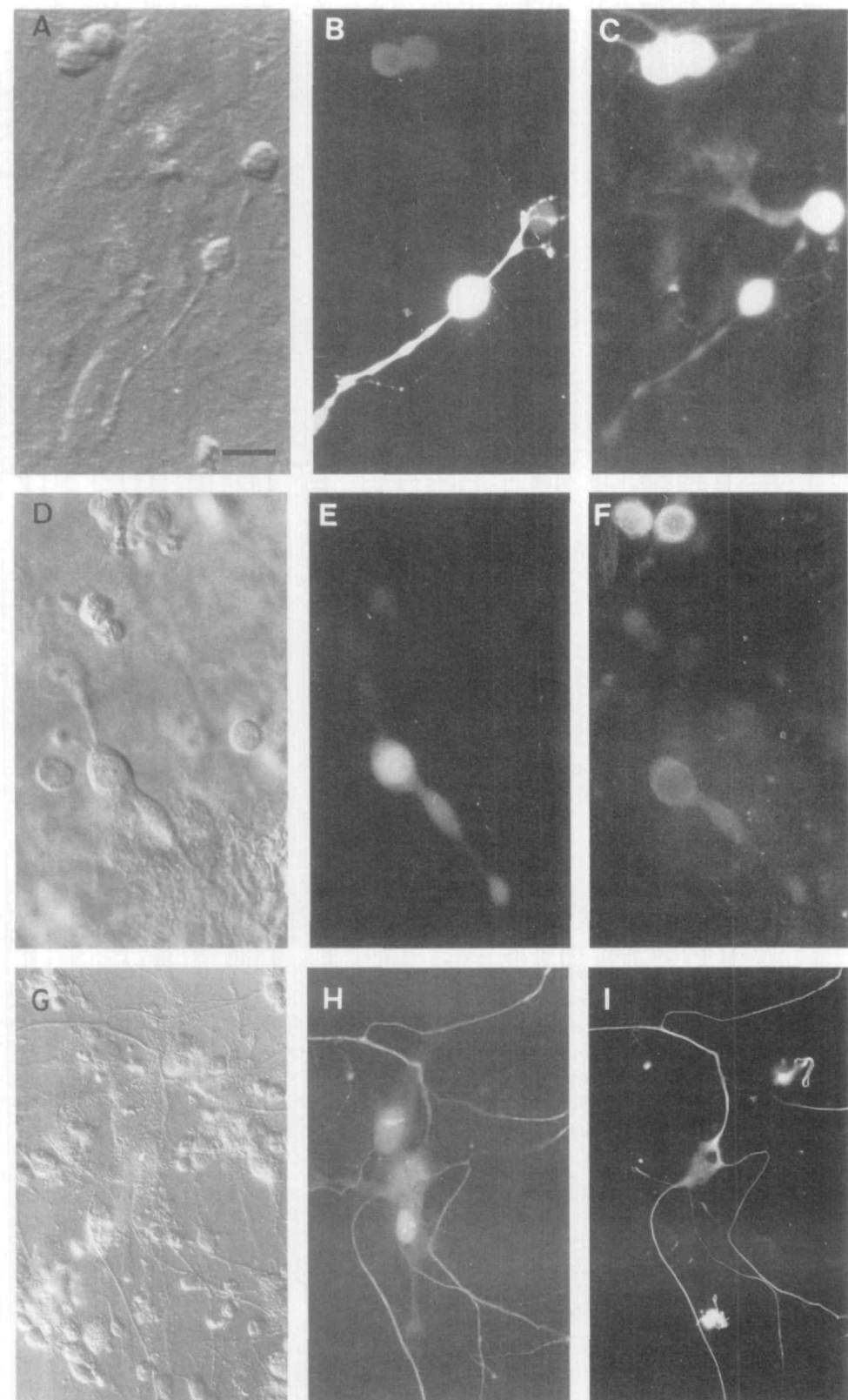


**FIGURE 4.** Immunocytochemical identification of recorded human cells in culture. (A, D, G) Nomarski differential interference contrast micrograph of human retinal cell cultures. (B, E) Fluorescence micrograph of the recorded cells stained with either sulforhodamine 101 (SR101; B, H) or Lucifer yellow (E). Sulforhodamine 101 produced red fluorescence under green excitation, whereas Lucifer yellow generated yellow fluorescence under blue excitation. (C, F) Staining with anti-parvalbumin antibody of the cultures. Recorded cells that presented the anomalous rectifier  $K^+$  current illustrated in Figure 3 were parvalbumin immunonegative. Their staining is less intense than other nonrecorded parvalbumin-immunopositive cells, an observation made in keeping with the partial washout of cytosolic parvalbumin during the recording. (I) Immunolabeling with anti-neurofilament antibody of

between  $-80$  mV and  $-50$  mV, with half inactivation at  $-61$  mV (Fig. 5A, square). The current varied from  $321$  pA to  $777$  pA ( $510 \pm 51$  pA,  $n = 10$ ) at  $+50$  mV after a conditioning stimulus at  $-120$  mV. These characteristics of the transient outward current are consistent with the presence of a  $I_A$  in human HCs.

### Delayed Rectifier $K^+$ Current

A sustained outward current was also observed at depolarized potentials when the inward anomalous rectifier  $K^+$  current and the transient outward  $K^+$  current were blocked by  $Cs^{2+}$  and 4-AP, respectively. This sustained outward current was suppressed by substituting  $30$  mM TEA for an equimolar concentration of NaCl in the bathing solution (Fig. 5B, inset). This TEA-sensitive current activated at potentials more positive than  $-40$  mV, and it increased linearly with the command voltage (Fig. 5B). The current varied from  $78$  pA to  $138$  pA at  $+50$  mV ( $110 \pm 9$  pA,  $n = 8$ ). This TEA-sensitive outward current is consistent with the presence of a delayed rectifier  $K^+$  current in human HCs.

### Calcium Current

Figure 5C illustrates the  $Ca^{2+}$  current measured in human HCs. For these measurements,  $K^+$  currents had been suppressed with  $5$  mM  $CsCl_2$ ,  $10$  mM 4-AP, and  $30$  mM TEA. Whole-cell currents were first measured in the presence of  $10$  mM  $CaCl_2$  to increase the  $Ca^{2+}$  current and, subsequently, in the presence of  $4$  mM  $CoCl_2$  to suppress it.  $Ca^{2+}$  current measurements were obtained by subtracting the cellular currents measured in either of these two conditions. The currents were sustained, activated at  $-10$  mV, and reached a maximum at  $+10$  mV or  $20$  mV. They were suppressed by ( $65.7\% \pm 3.1\%$ ,  $n = 3$ ) in the presence of nifedipine ( $10$   $\mu$ M). These features are consistent with the activation of an L-type  $Ca^{2+}$  current in human HCs.

### Sodium Current

In human HCs, no transient inward current, suggestive of a  $Na^+$  current, was obtained in most cases. The absence of a  $Na^+$  current was not related to the recording conditions, because cells with large transient inward currents (Figs. 1C, 1E, 1F) were recorded on the same culture. However, in three cases, putative HCs were observed to generate a transient inward current. The rare occurrence of these cells with such transient inward currents prevented us from characterizing this cell type further.

### Glutamate Response

Cultured human HCs generated sustained responses to glutamate application, reversing close to  $0$  mV (Fig. 6A). The current-voltage (IV) curve of these responses showed a barely null slope below  $-60$  mV (Fig. 6B) that suggested a complex response, possibly involving NMDA receptors as in catfish HCs.<sup>15</sup> Because the NMDA receptor is blocked by  $Mg^{2+}$  and because it requires glycine for its activation, we applied the glutamate agonists in a  $Mg^{2+}$ -free solution containing  $0.5$   $\mu$ M glycine from the local perfusion system. In human HCs, AMPA

and kainate both generated large inward currents at  $-70$  mV (Fig. 6C) that varied in amplitude from  $71$  pA to  $439$  pA ( $236 \pm 27$  pA,  $n = 15$ ) and from  $88$  pA to  $471$  pA ( $334 \pm 48$  pA,  $n = 8$ ), respectively. AMPA and kainate produced currents that became positive at positive potentials (Fig. 6D). The reversal potentials of the AMPA and kainate currents were close to  $0$  mV (AMPA:  $-1 \pm 1.4$  mV,  $n = 4$ ; kainate:  $-2.5 \pm 0.2$  mV,  $n = 4$ ) despite the fact that a pipette solution was used to obtain a calculated equilibrium potential for  $Cl^-$  ( $E_{Cl^-}$ ) at  $-30$  mV. These AMPA and kainate responses were suppressed in the presence of  $25$   $\mu$ M CNQX, an antagonist of the AMPA/kainate receptors coupled to cationic channels, by  $89\%$  ( $n = 6$ ) and by  $93\%$  ( $n = 4$ ), respectively (Fig. 6C). All these features of the AMPA/kainate responses were consistent with the notion that human HCs express kainate/AMPA receptors coupled to cationic channels.

NMDA ( $0.3$  mM) produced no effect at positive potentials even in the  $Mg^{2+}$ -free perfusion solution, whereas it generated a large sustained response at  $-100$  mV even in the presence of extracellular  $Mg^{2+}$  ( $1$  mM; Fig. 6E). The IV curve of the NMDA effect confirmed that this glutamate receptor agonist was not acting in HCs at a classic NMDA receptor (Fig. 6F, square). In fact, the IV curve was symmetrical to that of the anomalous rectifier  $K^+$  current that had been increased with a high  $K^+$  solution ( $40$  mM  $K^+$ , calculated equilibrium potential for  $K^+$  [ $E_K$ ] at  $-31$  mV; Fig. 6F, circle). This symmetry suggested a modulation of the anomalous rectifier  $K^+$  current by NMDA. Such a modulation was further supported by the absence of an NMDA response in the presence of  $Cs^{2+}$  (Figs. 6E, 6F) that blocked this voltage-dependent current in HCs (Fig. 3). The modulation of the anomalous rectifier  $K^+$  current amplitude by NMDA is highly reminiscent of a similar glutamate modulation of this voltage-dependent current in fish HCs.<sup>37</sup> In human HCs, glutamate also modulated the anomalous rectifier  $K^+$  current current. The response to glutamate application was greatly increased at  $-100$  mV in the presence of  $Cs^{2+}$  (Fig. 6E), and the IV curve of the glutamate effect became linear (Fig. 6G, square). These results indicated that the complex response to glutamate in human HCs is made up of both the activation of kainate/AMPA receptors and a modulation of the anomalous rectifier  $K^+$  current.

### GABA Receptors

GABA induced an inward current at  $-70$  mV that varied greatly in amplitude, from  $8$  pA to  $549$  pA ( $194 \pm 37$  pA,  $n = 22$ ; Fig. 7A). GABA responses were always suppressed in the presence of either bicuculline ( $0.2$  mM) or picrotoxin ( $0.2$  mM) by  $96\%$  ( $\pm 1.1\%$ ,  $n = 11$ ) and  $92\%$  ( $\pm 1.6\%$ ,  $n = 6$ ), respectively (Fig. 7A). Furthermore, the reversal potential of GABA responses was observed to follow approximately  $E_{Cl^-}$  ( $E_{Cl^-} = 0$  mV:  $E_{rev} = 2.8 \pm 2.5$  mV,  $n = 4$ ;  $E_{Cl^-} = -30$  mV:  $E_{rev} = -26.1 \pm 0.9$  mV,  $n = 4$ ; Fig. 7B). These results indicated that GABA responses were only or almost completely mediated by a  $GABA_A$  receptor in human HCs.

the culture. A recorded cell with extensive neuritic ramifications is double-labeled, whereas a glial cell that was filled with SR101 is clearly immunonegative. Scale bar, (A, B, C, D, E, F)  $13$   $\mu$ m; (G, H, I)  $25$   $\mu$ m.

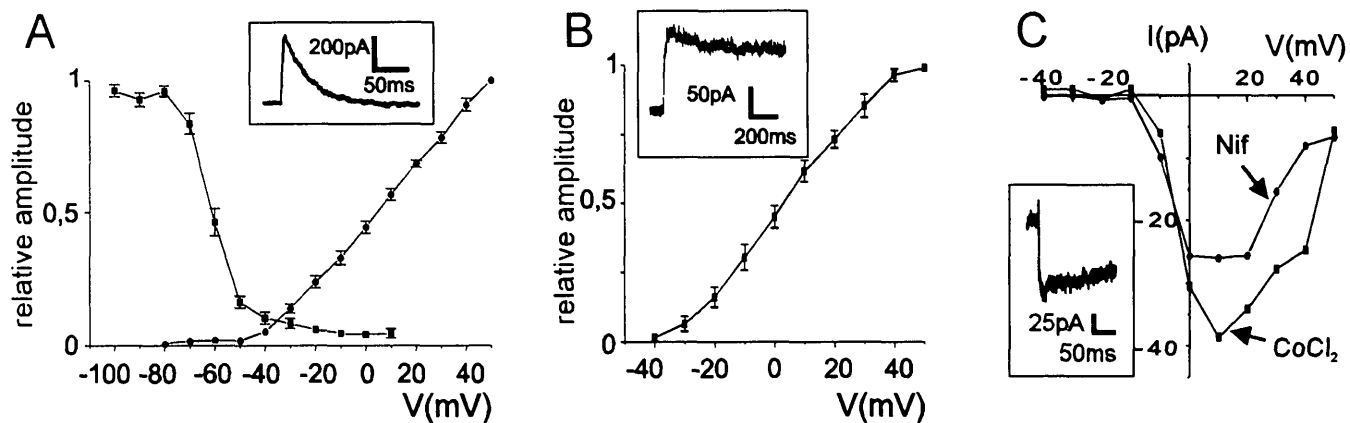


**FIGURE 5.** Voltage-gated currents in human horizontal cells. (A) Activation and inactivation curves of the transient outward  $K^+$  current. For the activation curve (circle,  $n = 9$  cells), the 4-aminopyridine (4-AP)-sensitive current was obtained by subtracting cellular currents measured in the absence or presence of 4-AP (10 mM) during voltage steps from a potential of  $-120$  mV in 10-mV increments. The inset illustrates the 4-AP-sensitive current when stepping to  $+50$  mV. The inactivation curve (square,  $n = 6$  cells) was calculated as in Löhrke and Hofmann<sup>9</sup> by measuring the 4-AP-sensitive current when stepping the cell to  $+50$  mV from conditioning potentials ranging from  $-120$  mV to  $+50$  mV. Measurements were normalized to the maximum in each cell and subsequently averaged. In these recordings, the anomalous rectifier  $K^+$  current was blocked with  $Cs^{2+}$  (5 mM). (B) The sustained outward  $K^+$  current. The TEA-sensitive current was obtained by measuring cellular currents in the absence or presence of tetraethylammonium (TEA, 30 mM) during voltage steps from a holding potential of  $-120$  mV. The inset illustrates the TEA-sensitive current measured in a cell when stepping the cell to  $+40$  mV. These measurements were made in the presence of  $Cs^{2+}$  (5 mM) and 4-AP (10 mM). TEA (30 mM) was exchanged for an equimolar concentration of NaCl. Measurements were normalized to the maximum in each cell and subsequently averaged. (C) L-type  $Ca^{2+}$  current. Current-voltage (IV) curves of the  $Ca^{2+}$  currents blocked by  $CoCl_2$  (4 mM) and those blocked by nifedipine (Nif; 10  $\mu$ M) in the same cell. The inset illustrates the current suppressed by  $CoCl_2$  during a voltage step from  $-70$  mV to  $+10$  mV. During the recordings, other voltage-gated conductances were blocked with  $Cs^{2+}$ , 4-AP, and TEA.

## Glycine Receptors

Glycine produced an inward current at  $-70$  mV that varied in amplitude from 135 pA to 1655 pA ( $763 \pm 269$  pA,  $n = 6$ ; Fig. 8A). These glycine responses were suppressed by 94% ( $\pm 4\%$ ,  $n = 6$ ) in the presence of strychnine (2  $\mu$ M), a classic blocker of glycine receptors (Fig. 8A). The reversal potential of the glycine response was found to follow approximately the calculated  $E_{Cl}$  ( $E_{Cl} = 0$  mV:  $E_{rev} = 1.3 \pm 1.4$  mV,  $n = 4$ ;  $E_{Cl} = -30$  mV:  $E_{rev} = -26.1 \pm 3.1$  mV,  $n = 3$ ; Fig. 8B). These results are in agreement with human HCs expressing a glycine receptor coupled to a  $Cl^-$  channel.

## DISCUSSION

Adult human retinal cells have been shown to survive and regenerate neurites for long periods of time in monolayer culture.<sup>23-26</sup> With different cell markers and electrophysiological criteria, we provide evidence that representative members of the major retinal cell populations that exist *in vivo* may remain among the small percentage of surviving cells. One cell type that exhibits the electrophysiological hallmark of HCs was characterized further. The anomalous rectifier  $K^+$  current can indeed be considered as an electrophysiological signature for HCs in the retina because HCs are the only cells in the retina in which it has been observed (see Ref. 27). Furthermore, we observed the modulation of this anomalous rectifier  $K^+$  current by glutamate as has been previously described in fish HCs.<sup>37</sup> This electrophysiological identification was confirmed by immunocytochemical labeling of the recorded cells using an anti-parvalbumin antibody, the specificity of which had been

initially verified on frozen sections of human retina (Figs. 1G, 1H). Although immunolabeling of recorded cells was sometimes less intense than that of nonrecorded HCs in the vicinity, we believe this was due to washout of parvalbumin, a cytosolic  $Ca^{2+}$ -binding protein, during the recording. The correspondence between electrophysiological and immunocytochemical criteria identified the cell type as human HCs.

This human HC population generated all the voltage-gated conductances classically observed in HCs from fish,<sup>3-6</sup> reptiles,<sup>7</sup> and mammals.<sup>8,9</sup> AMPA/kainate and GABA<sub>A</sub> receptors were also expressed, as has been observed in rabbits.<sup>16,38,39</sup> In contrast, we did not detect GABA<sub>C</sub> receptor or GABA transporter currents as in fish HCs.<sup>11-14</sup> In contrast to isolated A-type rabbit HCs,<sup>16</sup> all recorded human HCs also responded to glycine via a  $Cl^-$  channel-coupled receptor. The relative similarity of the results for human HCs to those obtained in other species supports the notion that retinal neurons preserve their basic physiological features during evolution, although the few differences underline the occurrence of a primate or human specificity.

## HC Populations

Parvalbumin antibodies were reported to label all HCs because they identify HI and HII in primate retinae and A- and B-type HCs in subprimate retinae.<sup>34</sup> In the human retina, one additional HC type has been subdivided from the HI type, on the basis of its size and connectivity.<sup>21</sup> These HIII HCs<sup>40</sup> may represent the parvalbumin-immunopositive cells in the INL that emit a process descending to the inner plexiform layer.<sup>34</sup> Therefore, it is unlikely that the parvalbumin immunoreactivity identifies a distinct HC population. Conversely, the anti-parval-

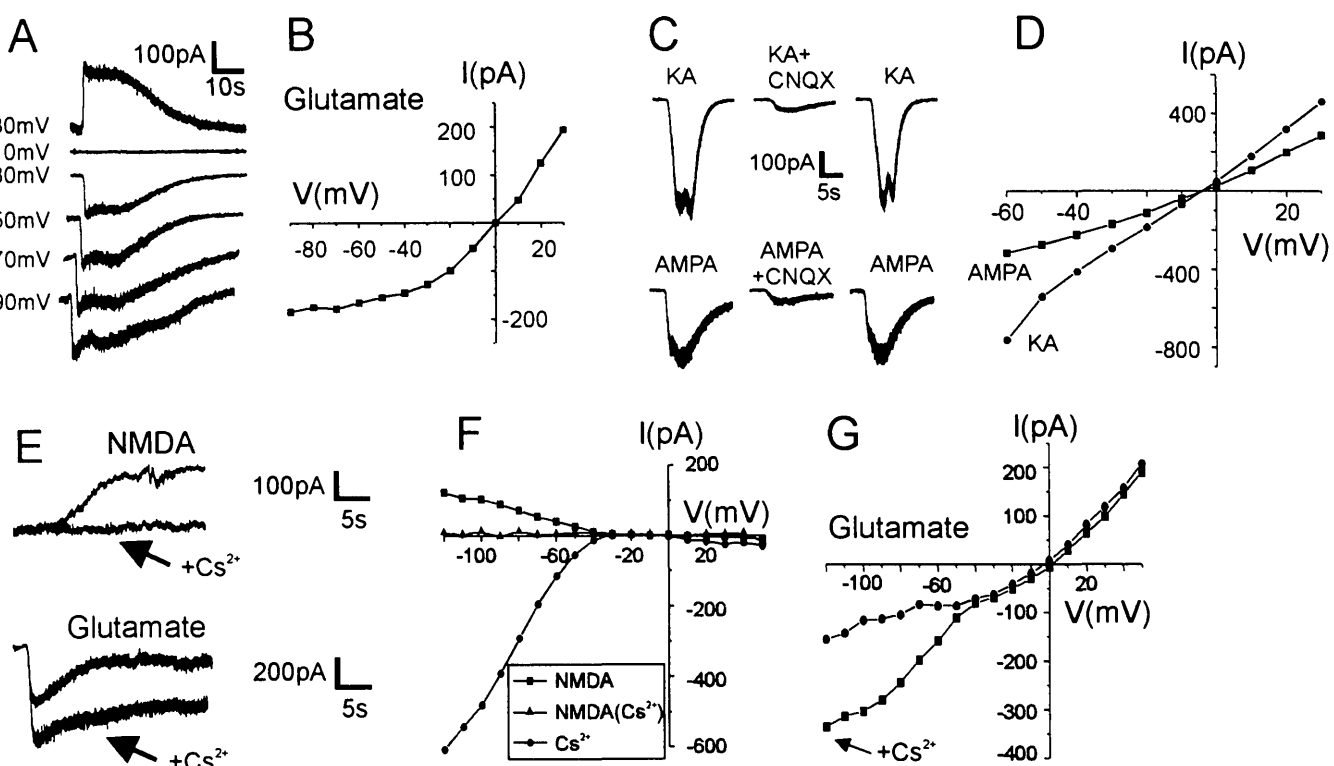


**FIGURE 6.** Responses to glutamate and its receptor agonist in human horizontal cells (HCs). (A) Responses to 5-second glutamate application (2 mM) at various potentials indicated at the left of the recording. The cell was recorded with the tetrapotassium intracellular solution ( $E_{Cl} = -30$  mV [where  $E_{Cl}$  is the equilibrium potential for  $Cl^-$ ]) and in a high  $K^+$  extracellular solution (40 mM  $K^+$ ). (B) Current-voltage (IV) curve of the maximum amplitude for the glutamate responses illustrated in (A). Note the null slope at potentials below -60 mV. (C) Sensitivity of kainate/(RS)- $\alpha$ -amino-3-hydroxy-5-methyl-4-isoxazolepropionic acid (AMPA) responses to 6-cyano-7-nitro quinoxaline-2,3-dione (CNQX; 25  $\mu$ M) in a human HC voltage-clamped at -70 mV. After the first application of the glutamate receptor agonist, CNQX was applied before and during the second application of the agonist. The response amplitude of the first application was recovered in a third application. The transient current at the peak of the kainate response was not consistently observed and appeared to be a perfusion artifact. (D) IV curves of the maximum amplitude of the kainate and AMPA responses from a cell voltage-clamped at various holding potentials. (E) N-methyl-D-aspartate (NMDA) and glutamate responses of human HCs voltage-clamped at -100 mV in the absence or presence of  $Cs^{2+}$  (10 mM) used to suppress the anomalous rectifier  $K^+$  ( $I_{anom}$ ) current. (F, G) IV curves of the NMDA- and glutamate-elicited currents in the same conditions as in (E). In contrast to the standard conditions (square), NMDA had no effect in the presence of  $Cs^{2+}$  (triangle). The IV curve of  $I_{anom}$  (circle in F;  $Cs^{2+}$ ) was presented to illustrate the symmetry with the NMDA-suppressed current (square) in the recording conditions ( $E_K = -31$  mV [where  $E_K$  is equilibrium potential for  $K^+$ ]). (G) The inward rectification of the glutamate-elicited current (circle) was suppressed in the presence of  $Cs^{2+}$  in the extracellular medium ( $Cs^{2+}$ , square). These measurements were obtained in voltage-step experiments applied from a holding potential of -20 mV (F) or 0 mV (G). In all recordings (E, F, G), cells were bathed in the high  $K^+$  solution (40 mM  $K^+$ ,  $E_K = -31$  mV).

bumin antibody also lightly stained cell bodies in the ganglion cells, and it cannot be excluded that anti-parvalbumin antibody also stained bipolar or amacrine cells, as suggested previously in the monkey retina.<sup>34</sup> However, we strongly believe that these neurons were not ganglion cells because cultured adult ganglion cells showed large inward  $Na^+$  currents as shown in Figure 1F.

In retinal cell cultures, parvalbumin-immunopositive cells were morphologically distinct from other immunocytochemically identified populations such as photoreceptors and bipolar cells (exhibiting essentially bipolar morphologies and limited neuritic extension) and amacrine and ganglion cells (with very highly developed process outgrowth; Figs. 1A, 1B, 1C, 1D). The small size of cultured HCs was consistent with the small cell body reported for human HCs *in situ*<sup>40</sup> and with the size of parvalbumin-immunopositive cell bodies at the outer part of the INL (Figs. 1H, 1I). Among HCs, however, observed differ-

ences in size and neurite branching patterns, and variations in capacitance measurement, were not sufficient to discriminate distinct HC subpopulations; these differences rather were ascribed to different eccentricities *in situ*. This difficulty to differentiate visually the HC subpopulations in culture was consistent with difficulties encountered in anatomic studies in differentiating HII from HI and HIII from HI cells.<sup>20,21,41</sup>

A- and B-type HCs from the cat retina differ in their voltage-dependent conductances by the amplitude of an L-type  $Ca^{2+}$  current and a transient outward  $K^+$  current. In our recording of human HCs, the amplitude of the voltage- and transmitter-gated currents varied from cell to cell, and no clear criterion enabled us to classify the cells into distinct cell populations. The absence of a  $Na^+$  current did not provide such a criterion because it has been reported to be sometimes absent from A-type mammalian HCs and sometimes present in B-type HCs.<sup>8-10</sup> Therefore, it remains unclear whether the present

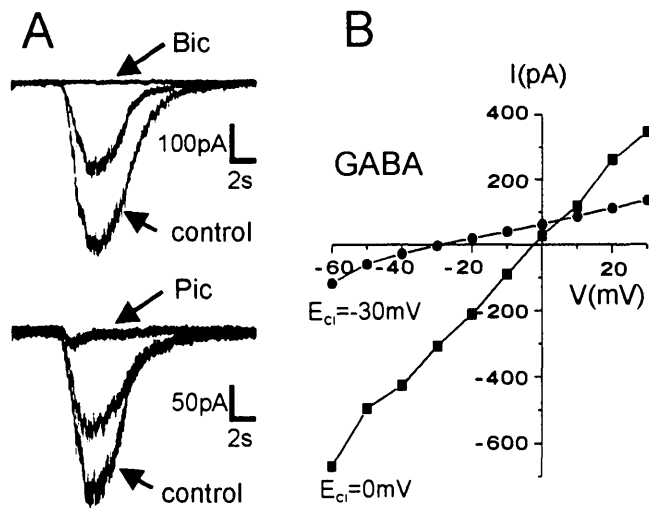


**FIGURE 7.**  $\gamma$ -Aminobutyric acid (GABA) responses in human horizontal cells. (A) Sensitivity of the GABA responses (0.1 mM, 5 seconds) to bicuculline (Bic; 200  $\mu\text{M}$ ) and picrotoxin (Pic; 200  $\mu\text{M}$ ) in a cell voltage-clamped at  $-70 \text{ mV}$ . After the first GABA response (control), either bicuculline or picrotoxin was applied before and during the second transmitter application. The response amplitude of the first application was partially recovered in a third application. (B) Current-voltage (IV) curves of GABA responses (0.1 mM, 5 seconds) in two cells with different recording pipette solutions to obtain a calculated equilibrium potential for  $\text{Cl}^-$  ( $E_{Cl}$ ) at either 0 mV or  $-30 \text{ mV}$ .

results refer to a single HC type or to a combination of the three different cell types. The inability to differentiate electrophysiologically each cell type might result from a relative homogeneity when processing the visual stimuli.<sup>22</sup> It is also highly possible that only one HC population had survived in culture or that only one HC population was visually selected during our experiments.

### Glutamatergic Input

Photoreceptors are generally considered to release glutamate in the human retina<sup>42,43</sup> as in other vertebrates.<sup>44</sup> This is consistent with the suppression of the light response in HCs by agonist (kainate, quisqualate) or antagonist applications of glutamate receptors in either lower vertebrates<sup>45-47</sup> or rabbits.<sup>38,39</sup> In human HCs, we demonstrated the presence of kainate/AMPA receptors. NMDA also generated an effect that could not be ascribed to the presence of a classic NMDA receptor as in catfish.<sup>15</sup> This result is consistent with the lack of expression for the NMDA receptor subunit NR2A in primate HCs.<sup>48</sup> NMDA and glutamate both appeared to modulate the anomalous rectifier  $K^+$  current in human HCs, as was described previously for glutamate in fish HCs.<sup>37</sup> The decrease of the anomalous rectifier  $K^+$  current by NMDA should only slow down the kinetics of the light response<sup>49</sup> and could not explain the hyperpolarizing effect of NMDA observed *in situ* on HCs.<sup>38,45</sup> The kainate/AMPA receptors in human HCs are consistent with the release of an excitatory amino acid transmitter by human photoreceptors.

### GABAergic Input

Horizontal cells are generally considered to release GABA by a carrier-mediated mechanism.<sup>50-53</sup> The HC transmitter in the

primate retinae appears also to be GABA as indicated by immunolabeling with either anti-GABA antibodies<sup>54-56</sup> or with antibodies directed against the GABA-synthesizing enzyme glutamic acid decarboxylase.<sup>54,57</sup> The suspected volatility of GABA in HCs<sup>56</sup> may explain the absence of immunoreactivity to GABA in human HCs; only a few processes were GABA-immunopositive in the OPL.<sup>21,43,58</sup> The lack of GABA transport current in rabbit A-type HCs<sup>16</sup> and human HCs (this study) together with the lack of immunoreactivity with anti-GABA transporter (GAT-1, GAT-2, and GAT-3) antibodies in rat HCs<sup>59,60</sup> raise questions about the carrier-mediated GABA release. However, these data are not sufficient to completely exclude this mechanism. First, currents generated by electrogenic transporters are rarely detectable in neurons because one or two charges are usually transferred per cycle; transporter-elicited currents can thus only be measured in high expression systems or after an amplification by a channel current. Second, mammalian HCs could express an unknown member of the GABA-transporter family.

Depending on the species studied, GABA responses in HCs are composed of different currents mediated by  $\text{GABA}_A^{12,16,18,19}$  and  $\text{GABA}_C^{11,12}$  receptors and GABA transporters.<sup>12-14</sup> In the human retina, the GABA-elicited current appeared to be exclusively or almost exclusively carried by a  $\text{GABA}_A$  receptor because picrotoxin and bicuculline both completely suppressed the current. This result is consistent with a study in rabbit A-type HCs in which the GABA response was also attributed solely to the  $\text{GABA}_A$  receptor.<sup>16</sup> However, it is quite surprising in view of the anti- $\text{GABA}_A$  receptor immunolabeling that is restricted to cone pedicles in the OPL of the cat and primate retinae.<sup>61-63</sup> The seeming discrepancy of these results may be explained by the fact that at the level of resolution used the immunostaining could also be postsynaptic and therefore in HC or, as noted by the authors, their antibodies might not recognize all forms of  $\text{GABA}_A$  receptors. The variability in GABA responses among human HCs may constitute a difference among HC populations, with one cell type perhaps

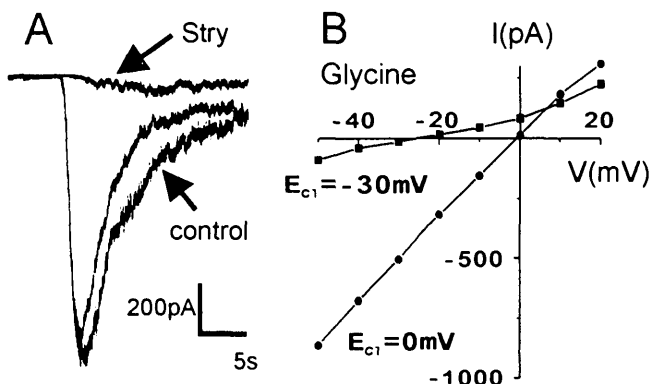


**FIGURE 8.** Glycine responses in human horizontal cells. (A) Sensitivity of the glycine responses (0.2 mM, 5 seconds) to strychnine (Stry; 2  $\mu\text{M}$ ) in a cell voltage-clamped at  $-70 \text{ mV}$ . After the first glycine response (control), strychnine was applied before and during the second transmitter application. The response amplitude of the first response was subsequently recovered in a third application. (B) Current-voltage (IV) curves of glycine responses in two cells with different recording pipette solutions to obtain a calculated equilibrium potential for  $\text{Cl}^-$  ( $E_{Cl}$ ) at either 0 mV or  $-30 \text{ mV}$ .

not expressing GABA receptors, as for HCs in the all-rod skate retina.<sup>13</sup>

### Glycinergic Input

Horizontal cells are sensitive to glycine in fish<sup>17</sup> and salamanders.<sup>18</sup> Interplexiform cells are usually considered the only glycinergic retinal neurons presynaptic to HCs,<sup>64</sup> although some bipolar cells also take up tritiated glycine and are immunolabeled by anti-glycine antibodies (see Ref. 65). In the primate retina, glycinergic interplexiform cells have not been described, and processes have been observed to ascend from the amacrine cell layer to the OPL only occasionally.<sup>66</sup> This occasional presence of glycine-containing neuronal processes in the OPL is associated with a sparse punctate distribution of glycine receptors.<sup>67</sup> Although infrequent, the presence of glycine and its receptors in the OPL is consistent with the glycine response generated in human HCs by glycine receptors. However, this glycinergic sensitivity appears to be a feature that is not common to all mammalian HCs, because rabbit A-type HCs did not respond to glycine despite the glycine sensitivity of their light response.<sup>16</sup> It is also possible that the pronounced glycine responsiveness results from culturing HCs. Taken together these studies point to a potential role of glycine in the OPL of the mammalian retina.

### Conclusions

This study represents the first comprehensive examination of voltage- and transmitter-gated channels in adult human HCs and more generally in a primate retinal neuron. Data generally concur with previous results in HCs from lower vertebrates and mammalian species, although differences in transmitter-gated currents were found when compared with rabbit HCs. These slight differences demonstrate the importance of studying the neuronal circuitry of the human retina. Adult retinal cell culture may therefore offer a novel and powerful model to characterize human retinal neurons and to develop new therapeutic approaches to blindness. Furthermore, this study demonstrates clearly that fully differentiated neurons can survive and regenerate neurites in vitro for extended periods.

### References

1. Werblin F. Synaptic connections, receptive fields, and patterns of activity in the tiger salamander retina: a simulation of patterns of activity formed at each cellular level from photoreceptors to ganglion cells. *Invest Ophthalmol Vis Sci*. 1991;32:459–483.
2. Kamermans M, Sprekpielse H. Spectral behaviour of cone-driven horizontal cells in teleost retina. In: Osborne N, Chader J, eds. *Progress in Retinal and Eye Research*. Oxford: Pergamon Press; 1995;14:313–360.
3. Tachibana M. Ionic currents of solitary horizontal cells isolated from goldfish retina. *J Physiol (Lond)*. 1983;345:329–351.
4. Lasater EM. Ionic currents of cultured horizontal cells isolated from white perch retina. *J Neurophysiol*. 1986;55:499–513.
5. Shingai R, Christensen BN. Excitable properties and voltage sensitive ion conductances of horizontal cells isolated from catfish (*Ictalurus punctatus*) retina. *J Neurophysiol*. 1986;56:32–49.
6. Malchow RP, Qian H, Ripps H, Dowling JE. Structural and functional properties of two types of horizontal cell in the skate retina. *J Gen Physiol*. 1990;95:177–198.
7. Golard A, Witkovsky P, Tranchina D. Membrane currents of horizontal cells isolated from the turtle retina. *J Neurophysiol*. 1992;68:351–361.
8. Ueda Y, Kaneko A, Kaneda M. Voltage-dependent ionic currents in solitary horizontal cells isolated from cat retina. *J Neurophysiol*. 1992;68:1143–1150.
9. Lörhke S, Hofmann HD. Voltage-gated currents of rabbit A- and B-type horizontal cells in monolayer cultures. *Vis Neurosci*. 1994;11:369–378.
10. Blanco R, Vaquero CF, De la Villa P. Action potentials in axonless horizontal cells isolated from the rabbit retina. *Neurosci Lett*. 1996;203:57–60.
11. Quian H, Dowling JE. Novel GABA responses from rod-driven retinal horizontal cells. *Nature*. 1993;361:162–164.
12. Dong CJ, Picaud SA, Werblin FS. GABA transporters and GABA<sub>A</sub>-like receptors on catfish cone- but not rod-driven horizontal cells. *J Neurosci*. 1994;14:2648–2658.
13. Malchow RP, Ripps H. Effect of  $\gamma$ -aminobutyric acid on skate retinal horizontal cells: evidence for an electrogenic uptake mechanism. *Proc Natl Acad Sci USA*. 1990;87:8945–8949.
14. Cammack JN, Schwartz EA. Ions required for the electrogenic transport of GABA by horizontal cells of the catfish retina. *J Physiol (Lond)*. 1993;472:81–102.
15. O'Dell TJ, Christensen BN. Horizontal cells isolated from catfish retina contain two types of excitatory amino acid receptors. *J Neurophysiol*. 1989;61:1097–1109.
16. Blanco R, Vaquero CF, De la Villa P. The effects of GABA and glycine on horizontal cells of the rabbit retina. *Vision Res*. 1996;36:3987–3995.
17. Zhou ZJ, Fain GL, Dowling JE. The excitatory and inhibitory amino acid receptors on horizontal cells isolated from the white perch retina. *J Neurophysiol*. 1993;70:8–19.
18. Yang XL, Wu SM. Effects of prolonged light exposure, GABA, and glycine on horizontal cell responses in tiger salamander retina. *J Neurophysiol*. 1989;61:1025–1035.
19. Stockton RA, Slaughter MM. Depolarizing actions of GABA and glycine on amphibian retinal horizontal cells. *J Neurophysiol*. 1991;65:680–692.
20. Kolb H, Mariani A, Gallego A. A second type of horizontal cell in the monkey retina. *J Comp Neurol*. 1980;189:31–44.
21. Kolb H, Linberg KA, Fisher SK. Neurons of the human retina: a Golgi study. *J Comp Neurol*. 1992;318:147–187.
22. Dacey DM, Lee BL, Stafford DK, Pokorny J, Smith VC. Horizontal cell of the primate retina: cone specificity without spectral opponency. *Science*. 1996;271:656–659.
23. Oka MS, Frederick JM, Lander RA, Bridges CDB. Adult human retinal cell in culture. *Exp Cell Res*. 1985;159:127–140.
24. O'Malley MB, MacLeish PR. Monoclonal antibody substrates facilitate long-term regenerative growth of adult primate retinal neurons. *J Neurosci Methods*. 1993;47:61–71.
25. Hicks D, Forster V, Dreyfus H, Sahel J. Survival and regeneration of adult photoreceptors in vitro. *Brain Res*. 1994;643:302–305.
26. Gaudin C, Forster V, Sahel J, Dreyfus H, Hicks D. Survival and regeneration of adult human and other mammalian photoreceptors in culture. *Invest Ophthalmol Vis Sci*. 1996;37:2258–2268.
27. Kaneko A, Tachibana M. Membrane properties of solitary retinal cells. In: Osborne N, Chader J, eds. *Progress in Retinal and Eye Research*. Oxford: Pergamon Press; 1986;5:125–146.
28. Fenwick EM, Marty A, Neher E. A patch clamp study of bovine chromaffin cells and of their sensitivity to acetylcholine. *J Physiol (Lond)*. 1982;331:577–597.
29. Grant GB, Werblin FS. Low-cost data acquisition and analysis programs for electrophysiology. *J Neurosci Methods*. 1994;55:89–98.
30. Hicks D, Courtois Y. Fibroblast growth factor stimulates photoreceptor differentiation in vitro. *J Neurosci*. 1992;12:2022–2033.
31. Wacker WB, Donoso LA, Kaslow CM, Yankeelov JA, Organisciak DT. Experimental allergic uveitis. Isolation, characterization, and location of a soluble uveitopathogenic antigen from bovine retina. *J Immunol*. 1977;119:1949–1958.
32. Negishi K, Kato S, Teranishi T. Dopamine cells and rod bipolar cells contain protein kinase C-like immunoreactivity in some vertebrate retinas. *Neurosci Lett*. 1988;94:247–252.
33. Wood JG, Hart CE, Mazzei GJ, Girard PR, Kuo JF. Distribution of protein kinase C immunoreactivity in rat retina. *Histochem J*. 1988;20:63–68.
34. Röhrenbeck J, Wässle H, Boycott BB. Horizontal cells in the monkey retina: immunocytochemical staining with antibodies against calcium binding proteins. *Eur J Neurosci*. 1989;1:407–420.

35. Barnstable CJ, Hofstein R, Akagawa K. A marker of early amacrine cell development in rat retina. *Dev Brain Res.* 1985;20:286-290.
36. Dräger UC, Edwards DL, Barnstable CJ. Antibodies against filamentous components in discrete cell types of the mouse retina. *J Neurosci.* 1984;4:2025-2042.
37. Kaneko A, Tachibana M. Effects of L-glutamate on the anomalous rectifier potassium current in horizontal cells of *Carassius auratus* retina. *J Physiol (Lond).* 1985;358:169-182.
38. Bloomfield SA, Dowling JE. Roles of aspartate and glutamate in synaptic transmission in rabbit retina, I: outer plexiform layer. *J Neurophysiol.* 1985;53:699-713.
39. Massey SC, Miller RF. Excitatory amino acid receptors of rod- and cone-driven horizontal cells in the rabbit retina. *J Neurophysiol.* 1987;57:645-659.
40. Kolb H, Fernandez E, Schouten J, Ahnelt P, Linberg KA, Fisher SK. Are there three types of horizontal cells in the human retina? *J Comp Neurol.* 1994;343:370-386.
41. Wässle H, Boycott BB, Röhrenbeck J. Horizontal cells in the monkey retina: cone connections and dendritic network. *Eur J Neurosci.* 1989;1:421-435.
42. Brandon C, Lam DMK. L-glutamic acid: a neurotransmitter candidate for cone photoreceptors in human and rat retinas. *Proc Natl Acad Sci USA.* 1983;80:5117-5121.
43. Marc RE, Lam DMK. Uptake of aspartic and glutamic acid by photoreceptors in goldfish retina. *Proc Natl Acad Sci USA.* 1981;78:7185-7189.
44. Davanger S, Ottersen OL, Strom-Mathisen J. Glutamate, GABA and glycine in the human retina: an immunocytochemical investigation. *J Comp Neurol.* 1991;311:483-494.
45. Rowe JS, Ruddock KH. Depolarization of retinal horizontal cells by excitatory amino acid neurotransmitter agonists. *Neurosci Lett.* 1982;30:257-262.
46. Lasater EM, Dowling JE, Ripps H. Pharmacological properties of isolated horizontal and bipolar cells from the skate retina. *J Neurosci.* 1984;4:1966-1975.
47. Yang XL, Wu SM. Effects of CNQX, APB, PDA, and kynurenone on horizontal cells of the tiger salamander retina. *Vision Neurosci.* 1989;3:207-212.
48. Hartveit E, Brandstätter JH, Dassoe-Pognetto M, Laurie DJ, Seuberg PH, Wässle H. Localization and developmental expression of the NMDA receptor subunit NR2A in the mammalian retina. *J Comp Neurol.* 1994;348:570-582.
49. Dong CJ, Werblin FS. Inwardly rectifying potassium conductance can accelerate the hyperpolarizing response in retinal horizontal cells. *J Neurophysiol.* 1994;74:2258-2265.
50. Schwartz EA. Calcium-independent release of GABA from isolated horizontal cells of the toad retina. *J Physiol (Lond).* 1982;323:211-227.
51. Schwartz EA. Depolarization without calcium can release  $\gamma$ -aminobutyric acid from a retinal neuron. *Science.* 1987;238:350-355.
52. Yazulla S, Kleinschmidt J. Carrier-mediated release of GABA from retina horizontal cells. *Brain Res.* 1983;263:63-75.
53. Ayoub GS, Lam DMK. The release of  $\gamma$ -aminobutyric acid from horizontal cells of the goldfish (*Carassius auratus*) retina. *J Physiol (Lond).* 1984;355:191-214.
54. Nishimura Y, Schwartz ML, Rakic P. Localization of  $\gamma$ -aminobutyric acid and glutamic acid decarboxylase in rhesus monkey retina. *Brain Res.* 1985;359:351-355.
55. Grünert U, Wässle H. GABA-like immunoreactivity in the macaque monkey retina: a light and electron microscopic study. *J Comp Neurol.* 1990;297:509-524.
56. Kalloniatis M, Marc RE, Murry RF. Amino acid signatures in the primate retina. *J Neurosci.* 1996;16:6807-6829.
57. Vardi N, Kaufman DL, Sterling P. Horizontal cells in cat and monkey express different isoforms of glutamic acid decarboxylase. *Vision Neurosci.* 1994;11:135-142.
58. Crooks J, Kolb H. Localization of GABA, glycine, glutamate and tyrosine hydroxylase in the human retina. *J Comp Neurol.* 1992;315:287-302.
59. Honda S, Yamamoto M, Saito N. Immunocytochemical localization of three subtypes of GABA transporter in rat retina. *Brain Res Mol Brain Res.* 1995;33:319-325.
60. Johnson J, Chen TK, Rickman DW, Evans C, Brecha NC. Multiple gamma-aminobutyric acid plasma membrane transporters (GAT-1, GAT-2, GAT-3) in the rat retina. *J Comp Neurol.* 1996;375:212-224.
61. Hughes TE, Carey RG, Vitorica J, De Blas AL, Kartner HJ. Immunocytochemical localization of GABA<sub>A</sub> receptors in the retina of the new world primate *Saimiri scuireus*. *Vision Neurosci.* 1989;2:565-581.
62. Hughes TE, Grünert U, Kartner HJ. GABA<sub>A</sub> receptors in the retina of the cat: an immunocytochemical study of wholemounts, sections and dissociated cells. *Vision Neurosci.* 1991;6:229-238.
63. Vardi N, Masarechia P, Sterling P. Immunoreactivity to GABA<sub>A</sub> receptor in the outer plexiform layer of the cat retina. *J Comp Neurol.* 1992;320:394-397.
64. Marc RE, Lam DMK. Glycinergic pathways in the goldfish retina. *J Neurosci.* 1981;1:152-165.
65. Marc RE. The role of glycine in the mammalian retina. In: Osborne N, Chader J, eds. *Progress in Retinal and Eye Research.* Oxford: Pergamon Press; 1989;8:67-107.
66. Hendrickson AE, Koontz MA, Pourcho RG, Sarthy PV, Goebel DJ. Localization of glycine containing neurons in the *macaca* monkey retina. *J Comp Neurol.* 1988;273:473-487.
67. Grünert U, Wässle H. Immunocytochemical localization of glycine receptors in the mammalian retina. *J Comp Neurol.* 1993;335:523-537.